

# Heat conduction in one dimensional systems: Fourier law, chaos, and heat control

Giulio Casati<sup>1,2</sup> and Baowen Li<sup>2</sup>

<sup>1</sup> Center for Nonlinear and Complex Systems, Università degli studi dell'Insubria, Como  
Istituto Nazionale di Fisica della Materia, Unità di Como, and  
Istituto Nazionale di Fisica Nucleare, sezione di Milano, Milano, Italy  
Giulio.Casati@uninsubria.it, phycg@nus.edu.sg

<sup>2</sup> Department of Physics, National University of Singapore, Singapore 117542,  
Republic of Singapore  
phylbw@nus.edu.sg

## 1 Introduction

"It seems there is no problem in modern physics for which there are on record as many false starts, and as many theories which overlook some essential feature, as in the problem of the thermal conductivity of nonconducting crystals" [1]. This statement by R. Peierls goes back to almost 50 years ago, yet it appears to be still valid. Compared with charge flow (electric current), much less is known about the heat flow.

Nevertheless, encouraging results have been obtained in recent years (see reviews [2] and the references therein). For example it is now known that in one dimensional systems of the Fermi-Pasta-Ulam (FPU) type [3], heat conduction is anomalous and the coefficient of thermal conductivity diverges with the system size  $L$  as  $L^{2=5}$  (when the transverse motion is considered  $L^{1=3}$  [4]). The connection between anomalous conductivity and anomalous diffusion has been also established [5, 6], which implies in particular that a subdiffusive system is an insulator in the thermodynamic limit and a ballistic system is a perfect thermal conductor, the Fourier law being therefore valid only when phonons undergo a normal diffusive motion. More profoundly, it has been clarified that exponential dynamical instability is a sufficient [7, 8] but not a necessary condition for the validity of Fourier law [9, 10, 11, 12]. These basic studies not only enrich our knowledge of the fundamental transport laws in statistical mechanics, but also open the way for applications such as designing novel thermal materials and/or devices such as the thermal rectifier [13, 14] and the thermal transistor [15].

In this paper we give a brief review of the relation between microscopic dynamical properties and the Fourier law of heat conduction as well as the connection between anomalous conduction and anomalous diffusion. We then discuss the possibility to control the heat flow.

## 2 Microscopic dynamics and the Fourier heat law

In spite of several years of investigation, so far there is neither phenomenological nor fundamental transport theory which can predict whether or not a given classical, many-body Hamiltonian system, yields an energy transport governed by the Fourier heat law. It is known that heat flow obeys a simple diffusion equation which can be regarded as the continuum limit of a discrete random walk. However, modern ergodic theory tells us that for K-systems, a sequence of measurements with finite precision mimics a truly random sequence and therefore these systems appear precisely those deterministically random systems tacitly required by transport theory. It is therefore interesting to establish which class, if any, of many-body systems satisfy the necessary stringent requirements for the validity of Fourier law of heat conduction.

### 2.1 Dynamical chaos is a sufficient condition for the Fourier law

#### Ding-a-ling model

The first example for which convincing evidence has been provided that Fourier law can be derived on purely dynamical grounds, without any additional statistical assumptions, is the so-called ding-a-ling model proposed in [7].

The Hamiltonian of the ding-a-ling model is:

$$H = \frac{1}{2} \sum_k p_k^2 + \sum_k \omega_k^2 q_k^2 + \text{hard point core} \quad (1)$$

where  $\omega_k$  equals  $\omega$  for even  $k$  and zero for odd  $k$  and where all particles have unit mass. It can be shown that it is possible to fix the energy per particle ( $E = 1$ ) and the half of the lattice distance between two bound particles ( $l_0 = 1$ ). After this the dynamics is uniquely determined by the frequency  $\omega$  which becomes therefore the only adjustable parameter.

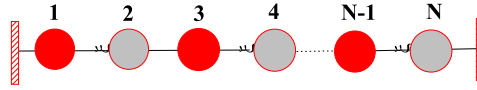


Fig. 1. The  $N$ -particle ding-a-ling model. Odd particles can move freely in between two collisions, while even particles are bounded by a harmonic spring.

As it seen in Fig 1, the model is a one-dimensional array of equal mass, hard-point particles, the even-numbered particles form a set of equally spaced harmonic oscillators with each oscillator bound to its individual lattice site

and with all oscillators vibrating with the same frequency  $\omega$ . The odd-numbered particles are free particles constrained only by the two adjacent even-numbered oscillators.

This model has been chosen in order to meet two requirements. First, it is necessary to select a deterministically random system, and second, the system must be sufficiently simple to allow efficient numerical analysis. Let us also recall that even systems obeying the Fourier heat law can transport energy in the form of slowly decaying coherent excitations such as soundlike pulses. In numerical experiments, which unavoidably consider only a small number of particles, this phenomenon is quite troublesome. Though K or almost K-system guarantees that these soundlike solutions will eventually decay, one needs to find a small chaotic system in which this decay rate is sufficiently rapid [16]. The selected model (1) is a many-body system which exhibits, as the frequency is varied, the full range of behaviour from integrable to almost K and which at the same time has no problem with energy-bearing, long-lived, solitonlike pulses. Indeed, it can be shown that as  $\omega$  is increased from zero (which is the well known integrable 1-d hard point gas), the system undergoes a transition from integrable to almost fully chaotic. This fact makes this model ideal to study the connection between Fourier law and microscopic dynamical chaos.

Heat conductivity has been studied by placing the end particles in contact with two thermal reservoirs at different temperatures (see [7] for details) and then integrating the equations of motion. Numerical results [7] demonstrated that, in the small  $\omega$  regime, the heat conductivity is system size dependent, while at large  $\omega$ , when the system becomes almost fully chaotic, the heat conductivity becomes independent of the system size (if the size is large enough). This means that Fourier law is obeyed in the chaotic regime.

#### Lorentz gas channel

The above conclusions have been nicely confirmed and clarified in [8] where the heat conduction has been studied in a Lorentz gas channel – a quasi one dimensional billiard with circular scatterers. The model (see Fig. 2) consists of two parallel lines and a series of semicircles of radius  $R$  placed in a triangular lattice along the channel. By construction no particle can move along the horizontal direction without colliding with the disks. The dynamics in the Lorentz gas is rigorously known to be mixing and all trajectories with nonzero projection on the horizontal direction are of hyperbolic type; further it has positive Kolmogorov-Sinai entropy and a well defined diffusive behavior. Very accurate numerical evidence has been provided [8] which shows that heat conduction in this model obeys the Fourier law. This result therefore clearly indicates that mixing with positive Lyapounov exponents is a sufficient condition to ensure Fourier law of heat conduction.



Fig. 2. The geometry of the Lorentz gas channel model. The two heat reservoirs at temperatures  $T_L$  and  $T_R$  are indicated.

## 2.2 Chaos is not a necessary condition

### Triangle billiard gas channel

Quite naturally, the next question which arises is whether strong, exponential unstable chaos, being sufficient, is also necessary.

In this connection let us remark that in spite of several efforts, the relation between Lyapounov exponents, correlations decay, diffusive and transport properties is still not completely clear. For example a model has been presented [17] which has zero Lyapounov exponent and yet it exhibits unbounded Gaussian diffusive behavior. Since diffusive behavior is at the root of normal heat transport then the above result [17] constitutes a strong suggestion that normal heat conduction can take place even without the strong requirement of exponential instability.

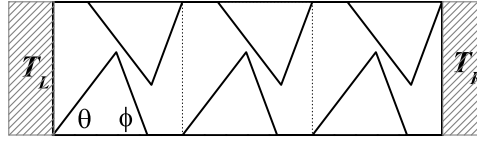


Fig. 3. The geometry of the triangle billiard gas channel. Particles move in the region outside the triangular scatterers. The two heat reservoirs at temperatures  $T_L$  and  $T_R$  are indicated.

The above problem has been addressed in [11], where we have considered a quasi-one dimensional billiard model which consists of two parallel lines and a series of triangular scatterers (see Fig.3). In this geometry, no particle can move between the two reservoirs without suffering elastic collisions with the triangles. Therefore this model is analogous to the previous Lorentz gas channel with triangles instead of discs: the essential difference is that in the triangular model the dynamical instability is linear and therefore the Lyapounov exponent is zero.

Strong numerical evidence has been given [18] that the motion inside a triangular billiard, with all angles irrational with  $\pi$  is mixing, without

any time scale. It is therefore reasonable to expect that the motion inside the irrational polygonal area of Fig 3 is diffusive thus leading to normal conductivity.

Indeed, numerical results in [11] show that in the irrational case (when the ratio  $\frac{M}{m}$  and  $\frac{M}{m}$  are irrational numbers) the system in Fig 3 exhibits normal diffusion and the heat conduction obeys the Fourier law. In the rational case instead, the system shows a superdiffusive behavior,  $\langle x^2 \rangle \sim t^{1.78}$  [11] and the heat conductivity diverges with the system size as  $\kappa \sim N^{0.25 \pm 0.01}$ .

#### Alternate mass-core hard potential channel

In the two billiard gas models just discussed there is no local thermalequilibrium. Even though the internal temperature can be clearly defined at any position [8], the above property may be considered unsatisfactory [19]. In order to overcome this problem, we have recently introduced a similar model which however exhibits local thermalequilibrium, normal diffusion, and zero Lyapunov exponent [12].

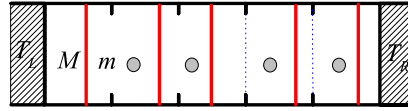


Fig. 4. The geometry of the alternate mass-core hard potential channel. The elementary cell is indicated by the two dotted lines. The bars have mass  $M = 1$ , and the particles have mass  $m = (\sqrt{5} - 1)/2$ . The two heat baths at temperatures  $T_L$  and  $T_R$  are indicated.

This model consists of a one-dimensional chain of elastically colliding particles with alternate masses  $m$  and  $M$ . In order to prevent total momentum conservation we confine the motion of particles of mass  $M$  (bars) inside separate cells. Schematically the model is shown in Fig.4: particles with mass  $m$  move horizontally and collide with bars of mass  $M$  which, besides suffering collisions with the particles, are elastically reflected back at the edges of their cells. In between collisions, particles and bars move freely.

Numerical results [12] clearly indicate that this model also obeys the Fourier law.

### 3. A normal Heat Conduction

Numerical experiments have shown that in many one dimensional systems with total momentum conservation, the heat conduction does not obey the

Fourier law and the heat conductivity depends on the system size. For example, in the so-called FPU model,  $L$ , with  $\alpha = 2=5$ , and if the transverse motion is introduced,  $\alpha = 1=3$ . Moreover, in the billiard gas channels (with conserved total momentum), the value of  $\alpha$  differs from model to model[5]. The question is whether one can relate  $\alpha$  to the dynamical and statistical properties of the system.

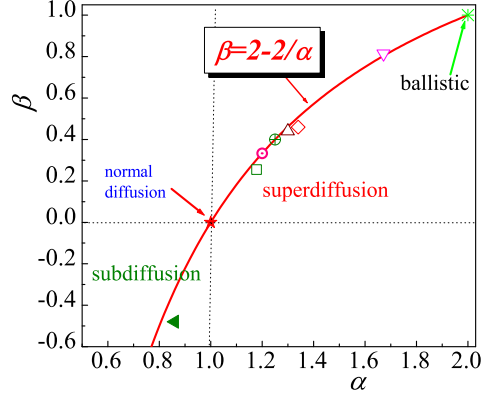


Fig. 5. Comparison of prediction (4) with numerical data. Normal diffusion (?). The ballistic motion (\*). Superdiffusion: 1D Ehrenfest gas channel[9](5); the rational triangle channel[11] (empty box); the polygonal billiard channel with  $\alpha_1 = (5-1)/4$ , and  $\alpha_2 = 3/4$  [10](4); the triangle-square channel gas[6] ( ). values are obtained from system size  $L \in [192; 384]$  for all channels except Ehrenfest channel[9]. The FPU lattice model at high temperature regime[6] ( ), and the single walled nanotubes at room temperature ( ). Subdiffusion: model from Ref.[10] (solid left triangle). The solid curve is  $\beta = 2 - 2/\alpha$ .

Recently, a simple formula has been found [5] which connects anomalous heat conductivity with anomalous diffusion. More precisely, it has been shown that for a one dimensional system, if the energy diffusion can be described by

$$\langle x^2 \rangle = 2D t^\alpha; \quad (0 < \alpha < 2) \quad (2)$$

then the heat conductivity is given by

$$\kappa = \frac{1}{L} \sum_j v_j^2 T / \alpha \quad (3)$$

where the exponent  $\alpha$  is

$$\alpha = 2 - 2/\beta \quad (4)$$

This relation connects heat conduction and diffusion, quantitatively. As expected, normal diffusion ( $\beta = 1$ ) corresponds to the size-independent

( $\alpha = 0$ ) heat conduction obeying the Fourier law. Moreover, a ballistic motion ( $\alpha = 2$ ) implies that the thermal conductivity is proportional to the system size  $L$ , a superdiffusive behavior ( $1 < \alpha < 2$ ) implies a divergent thermal conductivity ( $\alpha > 0$ ), and a subdiffusive behavior ( $\alpha < 1$ ) implies zero thermal conductivity ( $\alpha < 0$ ) in the thermodynamic limit.

The simple relation (4) is in good agreement with existing data from billiard gas channels to nonlinear lattices, and even single walled nanotubes[6]. This is shown in Fig. 5, where we compare the theoretical prediction (4) with existing data in different models.

We should mention here the one dimensional hard point gas model for which anomalous heat conduction has been found by several authors [20, 21]. However it seems there is no agreement on the numerical value of the exponent  $\alpha$ . Indeed in Ref.[20], the value  $\alpha = 0.25$  has been found, while the value  $\alpha = 0.33$  is reported in [21].

## 4 Control of heat flow

While in the previous sections we have discussed the relation between dynamical chaos and heat conductivity, in the following we will turn our attention to the possibility to control heat flow. Actually a model of thermal rectifier has been recently proposed [13] in which the heat can flow preferentially in one direction. Although this model is far away from a prototype realization, it is based on a mechanism of very general nature and, as such, is suitable of improvement and may eventually lead to real applications. This problem is discussed in the next section.

### 4.1 Thermal diode

In a recent paper [14], a thermal diode model has been proposed in which, even though the underlying physical mechanism is similar to the one in Ref. [13], there is a new crucial element which allows to improve the efficiency by more than two orders of magnitude.

The diode model consists of two segments of nonlinear lattices coupled together by a harmonic spring with constant strength  $k_{int}$  (see Fig. 6). Each segment is described by the (dimensionless) Hamiltonian:

$$H = \sum_i \frac{p_i^2}{2m} + \frac{1}{2}k(x_i - x_{i+1} - a)^2 - \frac{V}{(2\pi)^2} \cos 2\pi x_i; \quad (5)$$

The two ends of the system are put into contact with thermal baths at temperature  $T_L$  and  $T_R$  for left and right bath, respectively. In fact, Eq. (5) is the Hamiltonian of the Frenkel-Kontorova (FK) model which is known to have normal heat conduction [23]. For simplicity we set the mass of the particles and the lattice constant  $m = a = 1$ . Thus the adjustable parameters are

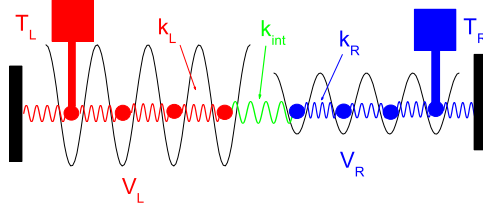


Fig. 6. Configuration of the thermally diode model based on two coupled FK chains.

$(k_L; k_{int}; k_R; V_L; V_R; T_L; T_R)$ , where the letter L/R indicates the left/right segment. In order to reduce the number of adjustable parameters, we set  $V_R = V_L$ ,  $k_R = k_L$ ,  $T_L = T_0(1 + \Delta)$ ;  $T_R = T_0(1 - \Delta)$  and, unless otherwise stated, we fix  $V_L = 5$ ,  $k_L = 1$  so that the adjustable parameters are reduced to four,  $(\Delta; k_{int}; T_0)$ . Notice that when  $\Delta > 0$ , the left bath is at higher temperature and vice versa when  $\Delta < 0$ .

In Fig. 7 we plot the heat current  $J$  versus  $\Delta$  for different temperatures  $T_0$ . It is clearly seen that when  $\Delta > 0$  the heat current ( $J_+$ ) increases with  $\Delta$ , while in the region  $\Delta < 0$  the heat current ( $J_-$ ) is almost zero, i.e. the system behaves as a thermal insulator. The results in Fig. 7 show that our model has the rectifying effect in a wide range of temperatures. The rectifying efficiency, defined as  $\eta = J_+/J_-$ , could be as high as few hundreds times, depending on temperature as well as on other parameters.

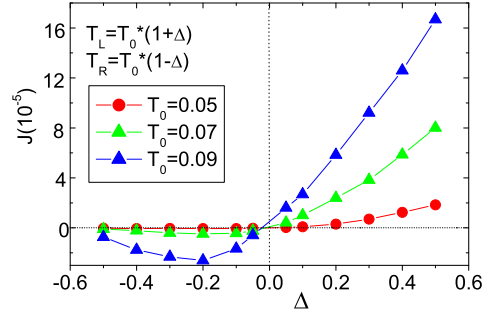


Fig. 7. Heat current  $J$  versus the dimensionless temperature difference  $\Delta$  for different values of  $T_0$ . Here the total number of particles  $N = 100$ ,  $k_{int} = 0.05$ ,  $\omega = 0.2$ . The lines are drawn to guide the eye.



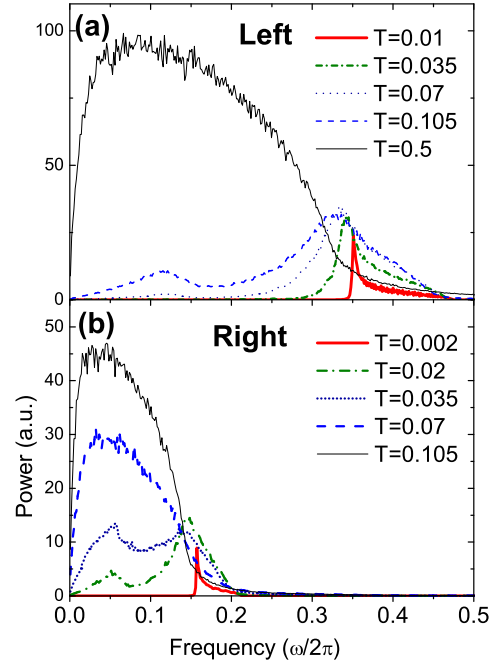


Fig. 8. Spectra of the two particles at the interface for different temperatures at  $k_{int} = 0$ . (a) particle at the left side of the interface, (b) particle at the right side of the interface. Here  $\gamma = 0.2$ ,  $N = 100$ .

#### Rectifying mechanism

To understand the underlying rectifying mechanism, let's start from the energy spectrum of the interface particles. Fig. 8 shows the phonon spectra of the left and right interface particles at different temperature when the two lattices are decoupled ( $k_{int} = 0$ ).

The match/mismatch of the energy spectra of the two interface particles controls the heat current. It is clearly seen from Fig. 8 that, if the left end is in contact with the high temperature bath  $T_L$ , and the right end with the low temperature bath  $T_R$  ( $T_R < T_L$ ), then the phonon spectra of the two particles at interface overlap in a large range of frequencies, thus the heat current can easily go through the system from the left end to the right end. However, if the left end is at lower temperature  $T_L$  and the right end is at higher temperature  $T_R$  ( $T_R > T_L$ ), then the phonon spectrum of the right interface particle is mainly in the low frequency part, while the left interface particle is in the high frequency part. Then there is almost no overlap in phonon frequency, and the heat current can hardly go through from right to

left, and the system behaves as an insulator. Why the left and right particles at the interface have so different phonon spectra? This can be understood from the following analysis on temperature dependent phonon spectra, due to the nonlinearity.

(1) Low temperature limit. At low temperature, the particle is confined in the valley of the on-site potential. By linearizing the equation of motion one can easily obtain the frequency band [14]:

$$\frac{P}{V} < \omega < \frac{P}{V + 4k}; \quad (6)$$

For the case of Fig. 7 with  $T = 0.01$  (left) and  $T = 0.002$  (right), this corresponds to  $0.36 < \omega < 0.48$  for the left particle and to  $0.16 < \omega < 0.21$  for the right particle.

As the temperature is increased, the interparticle potential  $kx^2/2$  becomes more and more important until a critical value  $T_{cr} = V/(2\beta)^2$  is reached (we take the Boltzmann constant equal unity), when the kinetic energy is large enough to overcome the on-site potential barrier. At this point low frequency appears and this happens at the critical temperatures  $T_{cr} = 0.13$  for  $V = 5$  (left), and  $T_{cr} = 0.025$  for  $V = 1$  (right). This is in quite good agreement with the data of Fig. 8.

(2) High temperature limit. In the high temperature limit the on-site potential can be neglected, the system is close to two coupled harmonic chains, and the phonon band is given by [24]:

$$0 < \omega < 2\sqrt{\frac{P}{k}}; \quad (7)$$

which gives  $0 < \omega < 0.32$  for the left particle and  $0 < \omega < 0.14$  for the right particle, again in good agreement with Fig. 8.

In fact, in order to optimize the rectifying effect, one should avoid the overlapping of the phonon bands in the low temperature limit (Eq. 6) and that in the high temperature limit (Eq. 7) for each segment of the system. According to the above estimates, one should have  $V > 4k$ , which is satisfied for the case of Fig. 8.

We should stress that it is the nonlinearity of the potential that makes phonon spectra temperature dependent, and thus the rectifying effect possible. Therefore it is reasonable to expect the rectifying effect to be present, in different degrees, in typical nonlinear lattices.

## 4.2 Negative Differential Thermal Conductance

Apart from the "one-way heat flow", the negative differential thermal resistance phenomenon observed in a certain temperature intervals in the thermal diode is of particular interest. As illustrated in Fig. 7 for  $\beta < 0.2$ , a smaller temperature difference ( $\Delta T$ ), can induce a larger heat current since, due to nonlinearity, it can result in a better match in phonon bands.

The same phenomenon is shown for different inter-face coupling constants  $k_{int}$  in Fig. 9 (a), and different system size in Fig. 9 (b).

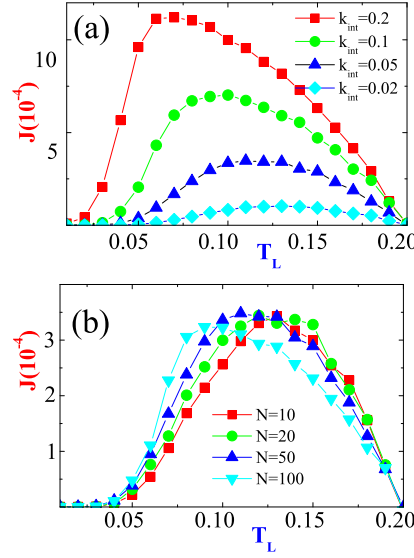


Fig. 9. (a) Heat current versus temperature  $T_L$  (at fixed  $T_R = 0.2$ ) for different coupling constants,  $k_{int}$ , with lattice size  $N = 50$ . The system parameters are:  $V_L = 5, V_R = 1, k_L = 1, k_R = 0.2$ . (b) Same as (a) but for different system size  $N$ .  $k_{int} = 0.05$ . Notice that when  $T_L \approx 0.1$  the heat current increases with decreasing the external temperature difference.

### 4.3 Thermal Transistor

The phenomenon of negative differential thermal resistance allows us to propose a "thermal transistor" [15]. The configuration of the thermal transistor is shown in Fig. 10 (a). It consists of three segments, D, S and G. The names D, S and G follow the ones used in a MOSFET (Metal-Oxide-Semiconductor Field-Effect-Transistor) that is the most important device for very large scale integrated chips such as microprocessors and semiconductor memories. Segment D (from D to O) has a negative differential thermal resistance in a certain temperature regime while segment S is a normal heat conductor, i.e., heat current inside this segment is positively dependent on temperature difference. Segment G is the control segment, which is connected to the junction particle between segments S and D. Temperature  $T_G$  will be used to control temperature  $T_O$  (at the junction O) so as to control the heat current from D to S. In analogy to the MOSFET, in which the electronic current in the electrode G is very small, we require here that the heat current  $J_G$  through segment G to be as small as possible, (otherwise it is hard to set  $T_G$  to a required value in experiment). Moreover the heat resistance of segment G must

be small enough in order to well control the temperature  $T_o$  by changing  $T_G$  so that  $T_o = T_G$ .

Notice that, in typical situations, the differential heat resistance,  $R_S = \frac{1}{\frac{\partial J_S}{\partial T_o}} \big|_{T_S = \text{const}}$  in segment S, and  $R_D = \frac{1}{\frac{\partial J_D}{\partial T_o}} \big|_{T_D = \text{const}}$  in segment D, are both positive and therefore there exists only one value of  $T_o$  for which  $J_S = J_D$  so that  $J_G = 0$ . Since  $J_S = J_D + J_G$ , the "current amplification factor",  $\beta = \frac{\frac{\partial J_D}{\partial J_G}}{\frac{\partial J_D}{\partial J_G}} = \frac{R_S}{R_S + R_D} < 1$ ; namely in order to make a change  $J_D$ , the control heat bath has to provide a larger  $J_G$ . This means that the "transistor" can never work!

The key point of our transistor model is the "negative differential heat resistance" as we observed in the diode model [14]. It provides the possibility that when  $T_o$  changes both  $J_S$  and  $J_D$  change simultaneously in the same way. Therefore  $J_S = J_D$  (or  $J_S = J_D$ ) can be achieved for several different values of  $T_o$  or even in a wide region of  $T_o$  as shown in Figs.10 and 11. In this situation heat switch and heat modulator/amplifier are possible. In the ideal, limiting case of  $R_S = R_D$  which, in principle, can be obtained by adjusting parameters, the transistor works perfectly.

#### Thermal Switch

We first demonstrate the "switch" function of our transistor, namely we show that the system can act like a good heat conductor or an insulator depending on the control temperature. This is illustrated in Fig.10 (b), where we plot  $J_G$ ;  $J_S$ , and  $J_D$  versus  $T_G$ . When  $T_G$  increases from 0.03 to 0.135, both  $J_D$  and  $J_S$  increase. In particular, at three points:  $T_G = 0.04; 0.09$  and  $0.135$ ;  $J_D = J_S$  thus  $J_G$  is exactly zero. These three points correspond to "off", "semi-on" and "on" states, at which  $J_D$  is  $2.4 \cdot 10^{-6}$ ;  $1.2 \cdot 10^{-4}$  and  $2.3 \cdot 10^{-4}$ , respectively. The ratio of the heat current at the "on" state and that at the "off" state is about 100, hence our model displays one important function - switch - just like the function of a MOSFET used in a digital circuit.

#### Thermal modulator/amplifier

As demonstrated above, the heat current from D to S can be switched between different values. However, in many cases, like in an analog circuit, we need to continuously adjust the current  $J_S$  and/or  $J_D$  in a wide range by adjusting the control temperature  $T_G$ . In Fig.11 we demonstrate this "modulator/amplifier" function of our transistor. The basic mechanism of such "modulator/amplifier" is the same as that of the "switch" but we consider here different parameter values. It is seen that in the temperature interval  $T_G \in (0.05; 0.135)$ , the heat current through the segment G remains very small ( $10^{-5}$  to  $10^{-5}$ ), within the shadow strip in Fig.10, while the heat currents  $J_S$  and  $J_G$  continuously increase from  $5 \cdot 10^{-5}$  to  $2 \cdot 10^{-4}$ .

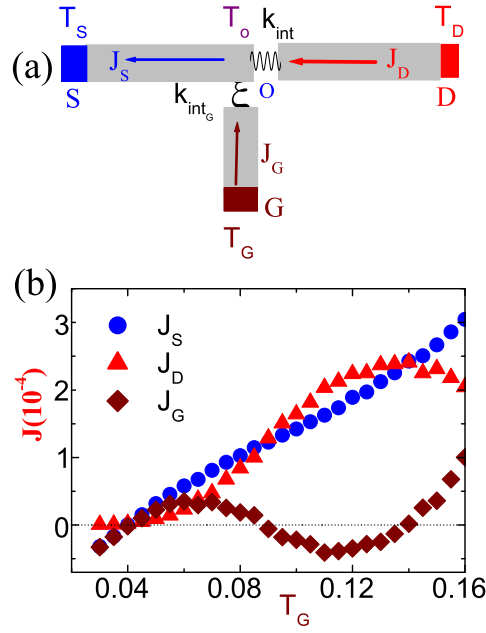


Fig. 10. (a) Configuration of the thermal transistor. (b) Heat current versus the control temperature  $T_G$ . Parameters are:  $T_D = 0.2$ ;  $V_D = 1.0$ ;  $k_D = 0.2$ ;  $k_{int} = 0.05$ ;  $T_S = 0.04$ ;  $V_S = 5$ ;  $k_S = 0.2$ ;  $V_G = 5$ ;  $k_G = 1$ ;  $k_{int_G} = 1$ . Notice that both  $J_S$  and  $J_D$  increase when the temperature  $T_G$  is increased.

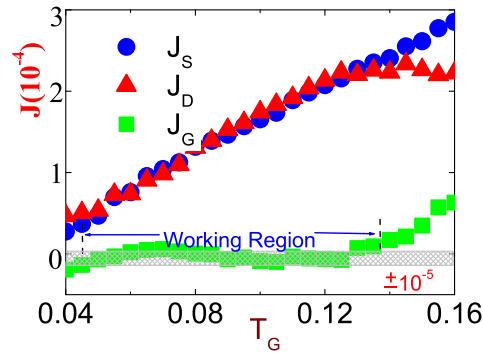


Fig. 11. Heat current versus the control temperature  $T_G$ . Here:  $T_D = 0.2$ ;  $V_D = 1.0$ ;  $k_D = 0.2$ ;  $T_S = 0.04$ ;  $V_S = 5$ ;  $k_S = 0.2$ ;  $k_{int} = 0.05$ ;  $V_G = 5$ ;  $k_G = 1$ ;  $k_{int_G} = 0.1$ . The shadow region is the range of variation of  $J_G$  in the temperature interval  $T_G \in (0.05; 0.135)$ .

## 5 Conclusions and discussions

In this paper, we have given a brief summary of our recent work on heat conduction in one dimensional systems. We have shown that strong chaos is sufficient but not strictly necessary for the validity of the Fourier heat law. Indeed linear mixing can be sufficient to induce a diffusive process which ensures normal heat conductivity.

For systems with total momentum conservation one typically finds anomalous conductivity, namely the thermal conductivity is divergent with the system size. Anomalous conductivity has been connected with anomalous diffusion via the very simple formula (4).

Finally we have shown the possibility to build a thermal diode which exhibits a very significant rectifying effect in a very wide range of system parameters. Moreover, based on the phenomenon of negative differential thermal resistance observed in the thermal diode, we have built a theoretical model for a thermal transistor. The model displays two basic functions of a transistor: switch and modulator/amplifier. Although at present it is just a model we believe that, sooner or later, it can be realized in a nanoscale system experiment. After all the Frenkel-Kontorova model used in our simulation is a very popular model in condensed matter physics [25].

## Acknowledgement

BL is supported in part by Faculty Research Grant of National University of Singapore and the Temasek Young Investigator Award of DSTA Singapore under Project Agreement POD 0410553. GC is partially supported by EU Contract No. HPRN-CT-2000-0156 (QTRANS) and by MURST (Prin 2003, Ordine caos nei sistemi estesi non lineari: strutture, stocasticita' debole e trasporto anomalo).

## References

1. R.E. Peierls, *Theoretical Physics in the Twentieth Century*, edited by M. Fierz and V.F. Weisskopf (Wiley, New York, 1961).
2. F. Bonetto et al., in *Mathematical Physics 2000*, A. Fokas et al. (eds) (Imperial College Press, London, 2000) (pp. 128-150); S. Lepri et al., *Phys. Rep.* 377, 1 (2003).
3. H. Kaburaki and M. Machida, *Phys. Lett. A* 181, 85 (1993); S. Lepri et al. *Europhys. Lett.* 43, 271 (1998); S. Lepri, *Phys. Rev. E* 58, 7165 (1998); S. Lepri et al., *Phys. Rev. Lett.* 78, 1896 (1997); B. Hu, B. Li, and H. Zhao, *Phys. Rev. E* 61, 3828 (2000); A. Pereverzev, *Phys. Rev. E*, 68, 056124 (2003).
4. J.-S. Wang and B. Li, *Phys. Rev. Lett.* 92, 074302 (2004); *Phys. Rev. E*, 70, 021204 (2004).

5. B. Li and J. Wang, Phys. Rev. Lett. 91, 044301 (2003); 92, 089402 (2004).
6. B. Li, J. Wang, L. Wang, and G. Zhang, CHAOS, xxx (2005); cond-mat/0410355.
7. G. Casati, J. Ford, F. Vivaldi, and W. M. Visscher, Phys. Rev. Lett, 52, 1861 (1984).
8. D. Alonso, R. Artuso, G. Casati, and I. Guameri, Phys. Rev. Lett 82, 1859 (1999).
9. B. Li, L. Wang, and B. Hu, Phys. Rev. Lett. 88, 223901 (2002)
10. D. Alonso et al, Phys. Rev. E 66, 066131 (2002).
11. B. Li, G. Casati, and J. Wang, Phys. Rev. E 67, 021204 (2003)
12. B. Li, G. Casati, J. Wang, and T. Prosen, Phys. Rev. Lett. 92, 254301 (2004)
13. M. Terraneo, M. Peyrard, and G. Casati, Phys. Rev. Lett 88, 094302 (2002).
14. B. Li, L. Wang, and G. Casati, Phys. Rev. Lett. 93, 184301 (2004).
15. B. Li, L. Wang, and G. Casati, cond-mat/0410173
16. B. V. Chirikov, Phys. Rep. 52, 263, 335 (1979).
17. G. Casati and T. Prosen, Phys. Rev. Lett. 85, 4261 (2000).
18. G. Casati, and T. Prosen, Phys. Rev. Lett. 83, 4729 (1999)
19. A. Dhar and D. Dhar, Phys. Rev. Lett. 82, 480 (1999).
20. A. Dhar, Phys. Rev. Lett., 86, 3554 (2001); G. Casati and T. Prosen, Phys. Rev. E 67, 015203(R) (2003).
21. P. Grassberger, W. Nadler, and L. Yang, ibid. 89, 180601 (2002); H. Li and H. Zhao, ibid 89, 079401 (2002).
22. J. Bardeen and W. H. Brattain, Phys. Rev. 74, 230 (1948).
23. B. Hu, B. Li, and H. Zhao, Phys. Rev. E 57, 2992 (1998).
24. C. Kittel, Introduction to Solid State Physics, 7<sup>th</sup> edition, John Wiley & Sons, Inc. (New York), 1996.
25. O. M. Braun and Y. S. Kivshar, Phys. Rep. 306, 1 (1998).